

Supplementary Information

Delocalization and bandgap engineering in defective MoS₂ by metal-ion doping for enhanced electrical performance and efficient near-infrared detection

Minho Yoon,^{a†*} Heung-Sik Kim,^{b†*} Jiyoul Lee,^{cd} Yong Uk Lee^{d*}

^aDepartment of Physics and Institute of Quantum Convergence Technology, Kangwon National University, Chuncheon, 24341, Republic of Korea

^bDepartment of Energy Engineering, Korea Institute of Energy Technology, Naju-si 58217, Republic of Korea

^cDepartment of Smart Green Technology Engineering, Pukyong National University, Yongso-ro 45, Nam-gu, Busan, 48513, Republic of Korea.

^dDepartment of Semiconductor Engineering, Division of Nanotechnology and Semiconductor Engineering, Pukyong National University, Yongso-ro 45, Nam-gu, Busan, 48513, Republic of Korea E-mail

† Minho Yoon and Heung-Sik Kim contributed equally to this work.

*Corresponding Author: E-mail: minhoyoon78@kangwon.ac.kr, jiyoul_lee@pknu.ac.kr, yongyong@pknu.ac.kr.

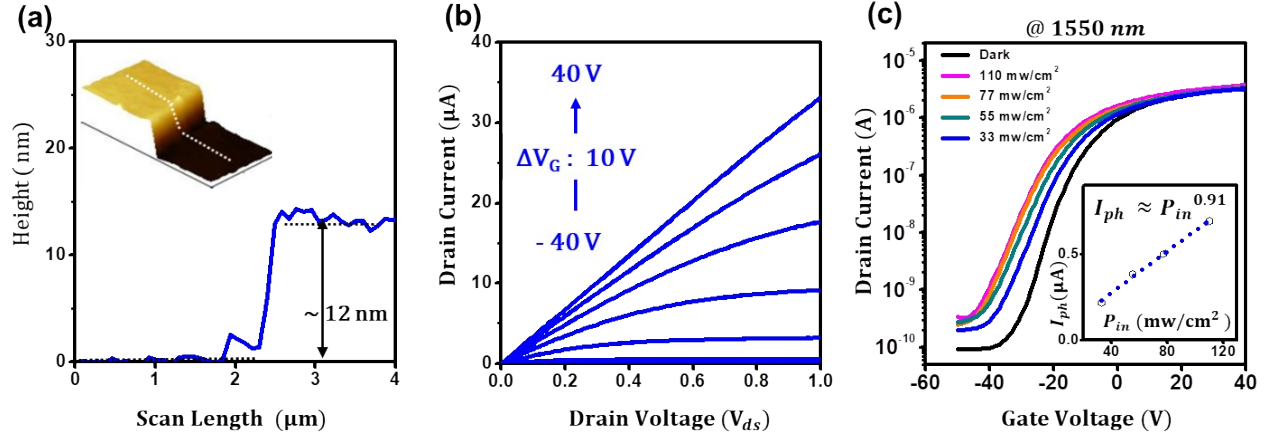


Fig. S1. (a) Thickness profiles (~ 12 nm) of the IGZO-coated MoS₂ FET. (b) The output characteristics (I_{ds} vs. V_{ds}) of the IGZO-coated MoS₂ FET. (c) Photo-response of the IGZO-coated MoS₂ FET as a function of power of the incident light. Inset: fitting curve with a power law.

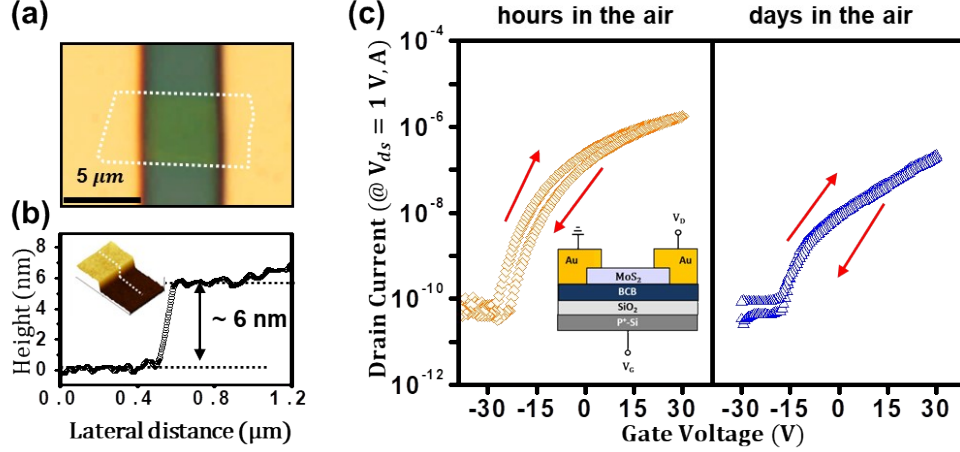


Fig. S2. (a, b) Optical microscopy (OM) image, AFM image along with channel thickness profiles (~ 6 nm). The channel width and length of the MoS₂ FET are 5.1 and 5.8 μm , respectively. (c) Transfer characteristics of n-type MoS₂ FET with 300 nm-thick BCB/SiO₂ dielectric with cross section scheme (inset).

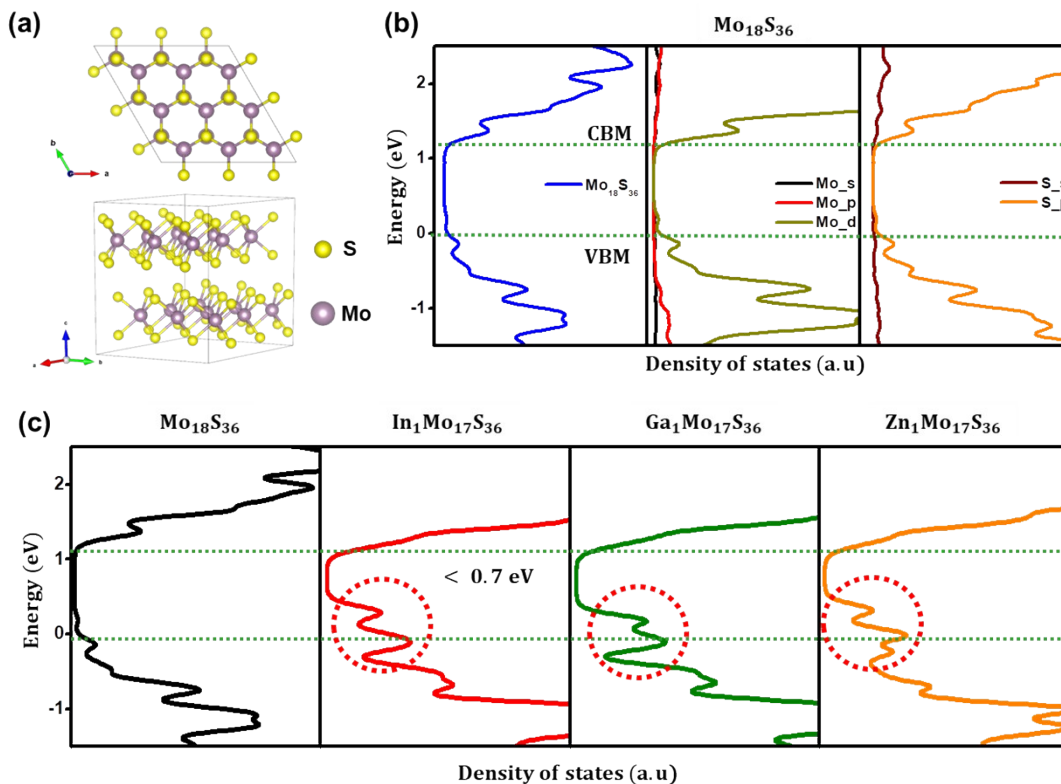


Fig. S3. (a) Constructed MoS₂ supercell. (b) Electronic density of states of MoS₂. (c) Electronic density of states of doped MoS₂ flakes, which contain metal ions such as indium (In), gallium (Ga), and zinc (Zn), respectively.

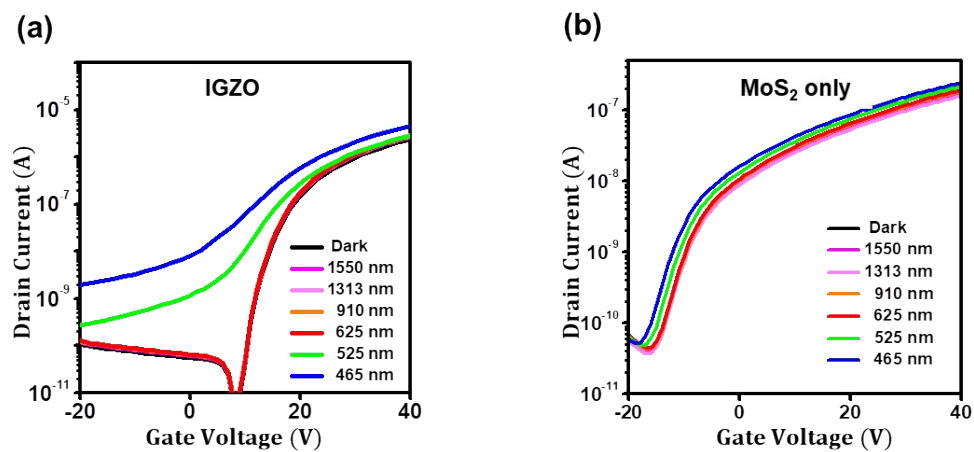


Fig. S4. (a, b) Photo-detecting properties of the IGZO and MoS₂ FET, respectively.

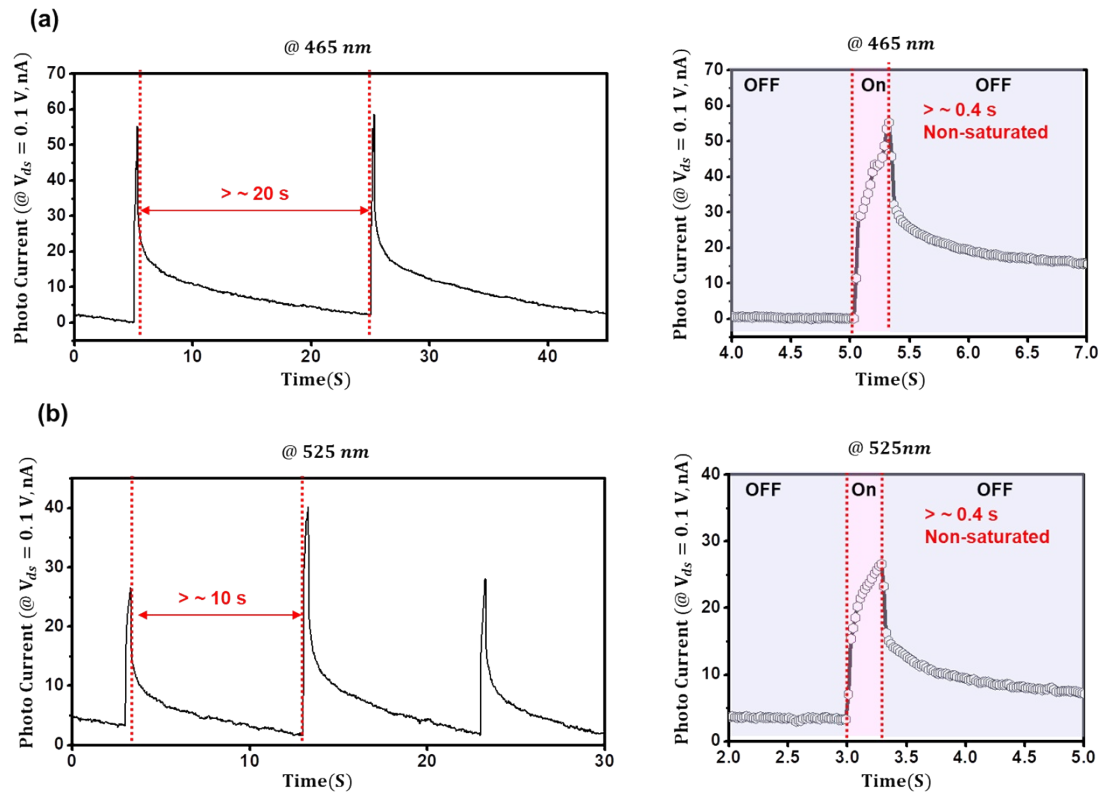


Fig. S5. (a, b) Dynamic photoresponse of the IGZO-coated MoS₂ phototransistor to visible lights (465 , 525 nm), respectively.

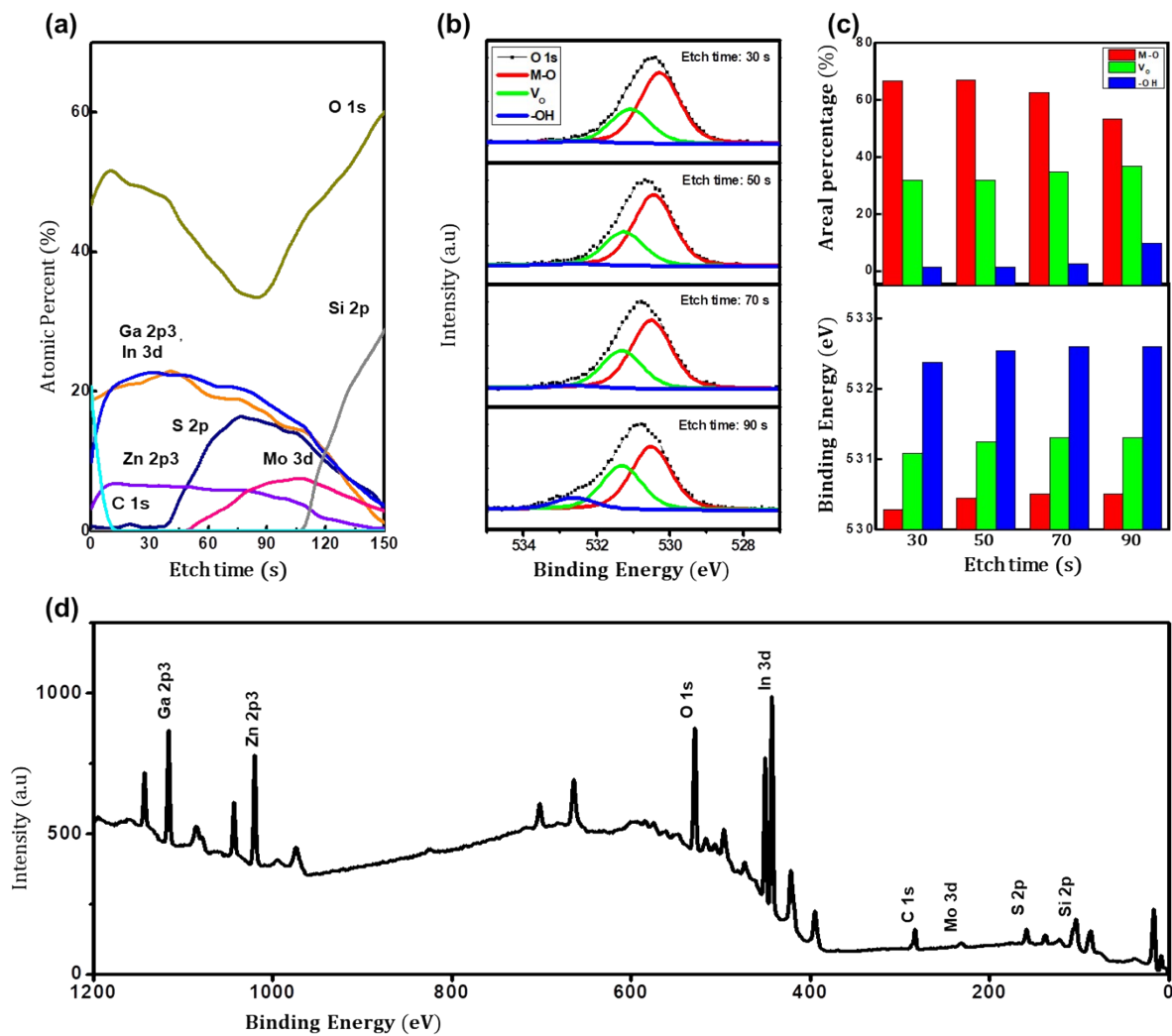


Fig. S6. XPS analyses of the IGZO-coated MoS₂. (a) XPS depth profile (b) O1s spectrum changes as a function of etch time. (c) Areal percentage and binding energy shift of O1s spectra. (d) Survey scan of the surface of the IGZO-coated MoS₂.

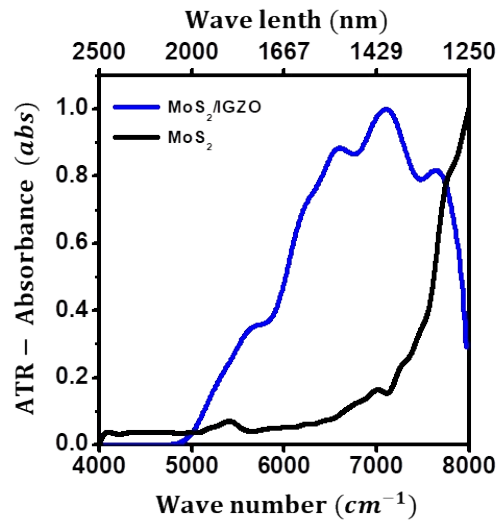


Fig. S7. Near-infrared absorption spectra of the MoS₂-only and MoS₂/IGZO flakes, respectively.

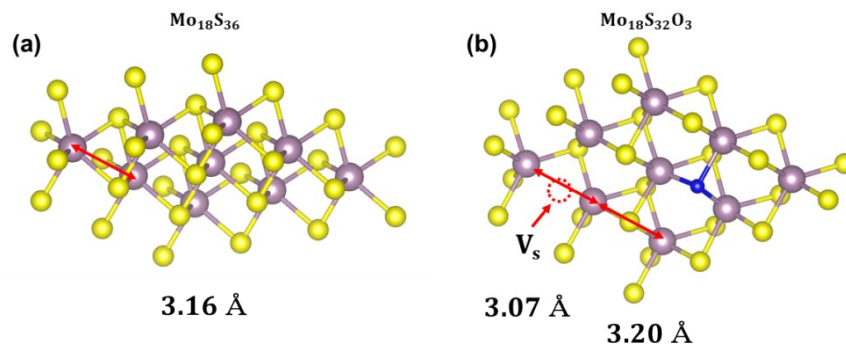


Fig. S8. (a, b) Fully relaxed crystal structure of MoS₂ and defective MoS₂, respectively.

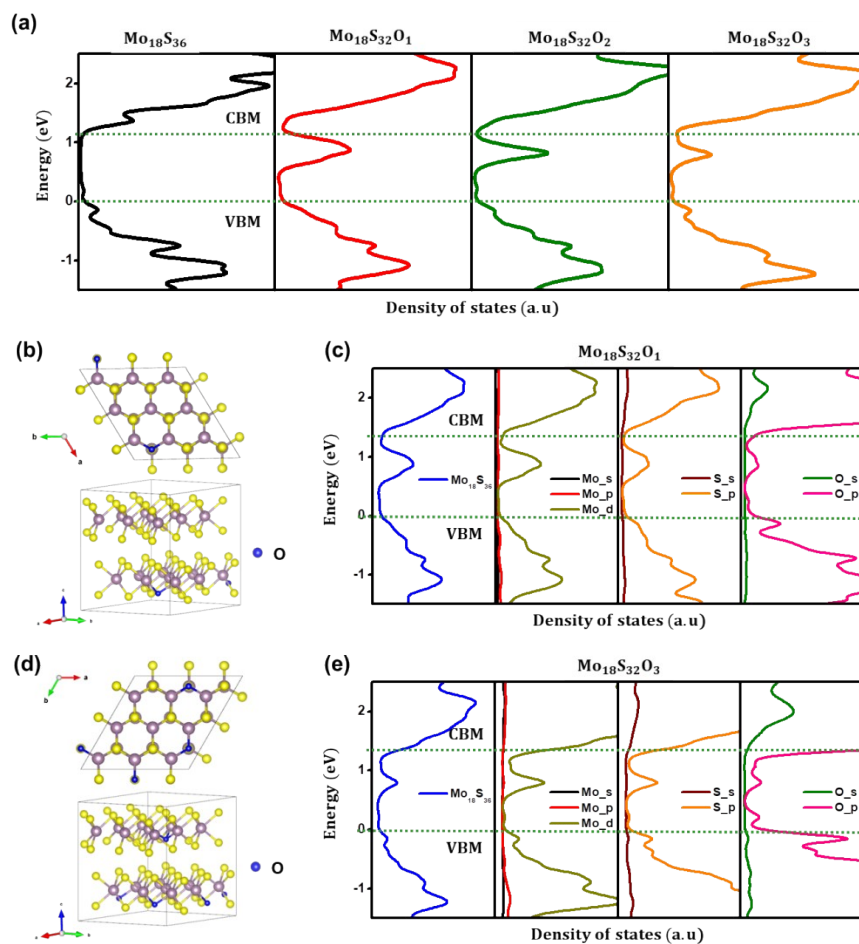


Fig. S9. (a) Electronic density of states of the defective MoS₂ according to the stoichiometry. (b, c) Constructed supercell and electronic density of states of defective MoS₂ (Mo₁₈S₃₂O₁). (d, e) Constructed supercell and electronic density of states of defective MoS₂ (Mo₁₈S₃₂O₃).

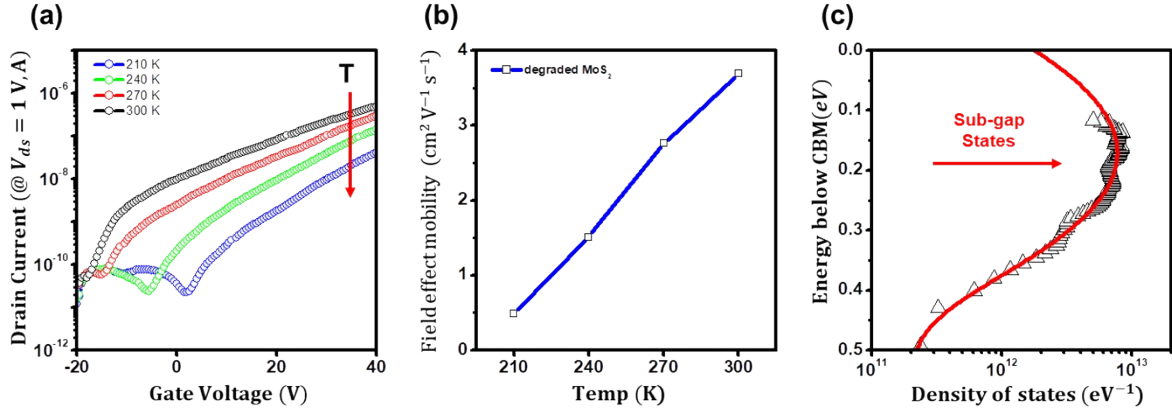


Fig. S10. (a, b) Temperature dependence of the transfer curves and field-effect mobility of the degraded MoS_2 FETs c Extracted charge trap density of states (DOS) of the degraded MoS_2 FET.